(2)

ARMY RESEARCH LABORATORY

Flamespreading in Granular Solid Propellant: Design of an Experiment

Douglas E. Kooker
Lang-Mann Chang
Stephen L. Howard

ARL-MR-80 June 1993

NOTICES

REPORT DOCUMENTATION PAGE

Form Approved
OMB No. 0704-0188

1. AGENCY USE ONLY *(Leave blank)*	2. REPORT DATE	3. REPORT TYPE AND DATES COVERED
	June 1993	Final, Jan 91 - Oct 92

4. TITLE AND SUBTITLE

Flamespreading in Granular Solid Propellant: Design of an Experiment

5. FUNDING NUMBERS

PR: 1L161102AH43

6. AUTHOR(S)

Douglas E. Kooker, Lang-Mann Chang, and Stephen L.Howard

7. PERFORMING ORGANIZATION NAME(S) AND ADDRESS(ES)

U.S. Army Research Laboratory
ATTN: AMSRL-WT-PE
Aberdeen Proving Ground, MD 21005-5066

8. PERFORMING ORGANIZATION REPORT NUMBER

9. SPONSORING/MONITORING AGENCY NAME(S) AND ADDRESS(ES)

U.S. Army Research Laboratory
ATTN: AMSRL-OP-CI-B (Tech Lib)
Aberdeen Proving Ground, MD 21005-5066

10. SPONSORING/MONITORING AGENCY REPORT NUMBER

ARL-MR-80

11. SUPPLEMENTARY NOTES

12a. DISTRIBUTION/AVAILABILITY STATEMENT

Approved for public release; distribution is unlimited.

12b. DISTRIBUTION CODE

13. ABSTRACT *(Maximum 200 words)*

When flamespreading in a gun system is rapid and reproducible, there is little incentive to improve our fundamental understanding of the ignition and flamespreading process. However, low-vulnerability (LOVA) propellants which are deliberately difficult to ignite can sometimes lead to anomalous ignition and flamespreading behavior. The present investigation is an attempt to study the fundamental behavior in a packed bed of granular gun propellant with a laboratory simulator. The apparatus consists of a hollow cylindrical pipe divided into two chambers. A small quantity of ball powder is burned in the igniter chamber sealed by a diaphragm and multiple-nozzle plate from the flow chamber which contains the sample granular solid propellant. Once the diaphragm bursts, combustion gases initially confined in the igniter chamber are driven through the nozzle plate forming a hot-gas planar wave which then propagates through the flow chamber. Behavior of this apparatus is discussed along with experimental pressure time-histories when the chamber is (a) empty and (b) filled with inert granular propellant. Results from a theoretical model help interpret some of the behavior.

14. SUBJECT TERMS

ignition, ignition studies, packed bed, flamespreading, solid propellants, simulators

15. NUMBER OF PAGES

34

16. PRICE CODE

17. SECURITY CLASSIFICATION OF REPORT	18. SECURITY CLASSIFICATION OF THIS PAGE	19. SECURITY CLASSIFICATION OF ABSTRACT	20. LIMITATION OF ABSTRACT
UNCLASSIFIED	UNCLASSIFIED	UNCLASSIFIED	UL

INTENTIONALLY LEFT BLANK.

TABLE OF CONTENTS

		Page
	LIST OF FIGURES	v
	ACKNOWLEDGEMENTS	vii
1.	INTRODUCTION	1
2.	BACKGROUND / CONVECTIVE IGNITION	1
2.1	Single Grain Experiments	2
2.2	Aggregate (Packed Bed) Experiments	3
3.	FLAMESPREADING CHAMBER EXPERIMENT	5
4.	MODEL OF THE FLAMESPREADING CHAMBER	11
5.	CONCLUDING REMARKS	18
6.	REFERENCES	19
	DISTRIBUTION LIST	21

INTENTIONALLY LEFT BLANK.

LIST OF FIGURES

Figure | Page

1. Schematic of flamespreading chamber apparatus 6

2. Schematic of igniter chamber/diaphragm system 7

3a. Igniter chamber/flow chamber pressure time-history; diaphragm failure 9

3b. Igniter chamber/flow chamber pressure time-history; successful diaphragm opening .. 9

4a. Flow chamber pressure time-history from the three wall-mounted gauges (from Figure 3b); successful diaphragm opening 10

4b. Pressure time-history on cylinder in shock tunnel as measured by Birk and Caveny (1980a, 1980b) 10

4c. Pressure time-history in modified shock tunnel as measured by Ritchie, Hsieh, and Kuo (1990a, 1990b) 10

5. Flow chamber pressure time-history from the three wall-mounted gauges; flow chamber contains inert granular propellant 11

6a. Model predictions for flamespreading chamber: igniter chamber pressure time-history [dash = isentropic flow through 100% of nozzle area, chain-dash = isentropic flow through 40% of nozzle area, solid = 1-ms delay opening of 40% nozzle area (A_{on} in cm^2 here)] 13

6b. Model predictions for flamespreading chamber: typical pressure time-history [solid = igniter chamber, chain-dash = flow chamber, dash = mass of ball powder remaining in igniter chamber]. Note: mass remaining (grams) is plotted on same scale as chamber pressure 13

7a. Model predictions for flow chamber pressure time-history. Combustion of 5-g ball powder in igniter chamber. Influence of diaphragm burst pressure: chain-dash = 10 MPa, solid = 15 MPa, chain-dot = 20 MPa. Calculation assumes zero time delay in nozzle opening 14

7b. Model predictions for flow chamber pressure time-history. Diaphragm burst pressure is 15 MPa. Influence of mass of ball powder burned in igniter chamber: solid = 5 g, chain-dash = 6 g, dot = 7 g. Calculation assumes zero time delay in nozzle opening 14

8a. Comparison of model predictions/data from Run #14: pressure time-history in igniter chamber. Burst pressure = 13 MPa, 1.5 ms delayed opening of 40% nozzle area (solid = igniter chamber, chain-dash = flow chamber) 15

8b. Comparison of model predictions/data from Run #14: pressure time-history in flow chamber (no granular solids). Burst pressure = 13 MPa, 1.5-ms delayed opening of 40% nozzle area (chain-dash = isothermal nozzle, dash = adiabatic nozzle) 15

9a. Comparison of model predictions/data from Run #31: pressure time-history in igniter chamber. Burst pressure = 17 MPa, 1.5-ms delayed opening of 40% nozzle area (solid = igniter chamber, chain-dash = flow chamber) 16

9b. Comparison of model predictions/data from Run #31: pressure time-history in flow chamber (no granular solids). Burst pressure = 17 MPa, 1.5-ms delayed opening of 40% nozzle area (chain-dash = isothermal nozzle, dash = adiabatic nozzle) 16

10. Comparison of model prediction/data from Run #35: pressure time-history in flow chamber (WITH inert granular solids). Burst pressure = 17.5 MPa, flow chamber volume = 800 cm^3 (chain-dash = isothermal nozzle, dash = adiabatic nozzle) 17

ACKNOWLEDGEMENTS

The authors would like to thank M. B. Ridgely and T. E. Rosenberger of the U. S. Army Research Laboratory (ARL) for their special assistance to this program at the ARL Indoor Range facility. The authors are also grateful to H. A. McElroy of the Olin Ordnance Corporation who, under the provisions of an ARL-Olin unfunded study agreement, supplied the ball powder propellant used in the igniter chamber.

INTENTIONALLY LEFT BLANK.

1. INTRODUCTION

During the early stage of the gun interior ballistic cycle, the crucial process is the propagation of an ignition front or "flame zone" through the packed bed of unburned propellant grains or sticks. Few concerns arise as long as the flamespreading process is rapid and reproducible. However, if the solid propellant happens to be difficult to ignite (e.g., low vulnerability propellant), or if the strength of the ignition system is marginal, significant delays can arise in the propagation of flame through the propellant bed. Delays in flamespreading often lead to combustion chamber conditions which promote large amplitude pressure waves (e.g., Horst [1983]). Diagnosing and correcting anomalous behavior associated with ignition and flamespreading would be much easier with a better understanding of the entire process.

In most gun systems, the convective ignition process is dominated by a three-dimensional flow field as the result of bayonet primers, tapered chamber walls, protruding projectile bases, etc. In this situation, it is virtually impossible to isolate and study only the flamespreading event. The present investigation is a deliberate attempt to remove the complicated three-dimensional geometry by looking at convective ignition in a simple laboratory device where the igniter drives an approximately planar wave through the confined bed of granular propellant. It is hoped that the thermal and pressure environment will replicate that of a typical gun combustion chamber (e.g., the 105-mm simulator of Chang and Rocchio [1988]). The pressure environment should also be similar to that created by previous shock tube experiments (see Section 2, below), but possibly without some of the harshness during the initial transient.

A primary focus of this investigation is directed toward low vulnerability propellants, which are often referred to as LOVA propellants. The reduced vulnerability to various hostile threats is often associated with (a) a higher threshold for thermal ignition, and (b) lower burning rates at low pressure. However, these very properties can also create difficulties in the ignition sequence of the gun system as discussed, for example, by Horst (1983). Since in many ways, the propagation of a convective ignition front through a bed of granular energetic material is poorly understood, it is not surprising that theoretical descriptions in various interior ballistic models are rather elementary. It is hoped that a database from the present experiment may be helpful in validating improved models.

2. BACKGROUND / CONVECTIVE IGNITION

A number of previous studies have found several important characteristics associated with convective ignition of energetic solid materials including LOVA propellant. The experiments seem to divide naturally into two categories, depending on whether the investigation involved a single grain of material or an aggregate (packed bed).

2.1 Single Grain Experiments. Birk and Caveny (1980a, 1980b) conducted an extensive series of ignition tests on various single cylinders (plus a tandem configuration) mounted transverse to the transient cross-flow created by diaphragm rupture in a shock tunnel. Depending upon the flow conditions imposed on the cylinder, the location or site of ignition could vary from the front stagnation region, the flow separation region, to the rear stagnation region in the cylinder wake. An important result is illustrated by Figure 55 in Birk and Caveny (1980a) which shows a plot of time to ignition versus freestream Reynolds number for a triple-base propellant (M30) in a flow of 100% nitrogen. It is quite likely that changes in the site of ignition are the cause of the non-monotonic structure of this curve. Note that when the freestream Reynolds number exceeds approximately 16,000, no ignition is observed. Even more important, a single-base propellant (M1), a double-base propellant (M26 with 25% NG), and a nitramine composite (85% HMX in a polyurethane binder) *would not ignite at any Reynolds number* in a flow of 100% nitrogen. However, when the composition of the freestream flow was altered to include 50% oxygen, all four materials ignited easily at Reynolds numbers less than 10,000. Note that Birk and Caveny's results for the nitramine composite HMX/PU are actually the first ignition data on what could be termed a prototype LOVA propellant.

If successful ignition merely involved raising the temperature of a certain fraction of material above some threshold value, then increasing the magnitude of the Reynolds number which increases the rate of convective heat transfer (presumably proportional to some power of Reynolds number) should shorten ignition delay times. Clearly it is not that simple for the materials studied by Birk and Caveny (1980a, 1980b). Their results illustrate the important concept of a Damkohler number (i.e., the ratio of a flow residence time to a characteristic time for reaction). Rapid ignition then implies a Damkohler number greater than unity. The Birk and Caveny data suggest that a minimum flow residence time is required. And furthermore, the addition of oxidizer to the freestream flow substantially decreases the characteristic time of the controlling reaction which is apparently in the gas phase. Unfortunately, identifying the controlling reaction (or reaction system) is not so simple. However, the one common feature shared by all the materials which will not ignite in 100% nitrogen is a prominent two-stage flame structure during combustion at low pressures (Miller 1992). Miller's photographs of the quasi-steady flame zone associated with various propellant samples in a strand burner at 2 MPa, for example, show evidence of an extended secondary flame zone (some distance above the regressing interface) for nitramine composites and single- and double-base propellants. The triple-base propellant, M30, by way of contrast, is characterized by a more vigorous flame zone at and near the regressing solid surface.

Ritchie, Hsieh, and Kuo (1990a, 1990b, 1992) modified the test section of the Birk and Caveny apparatus and then undertook similar experiments on single cylinders of the LOVA propellant XM-39 (76% RDX, 12% CAB, 7.6% ATEC, 4% NC, and 0.4% EC). Over the Reynolds number range of 30,000 to 50,000, all tests performed in 100% nitrogen showed no evidence of ignition or luminous flame. Recall that Birk and Caveny (1980) found a similar result for their nitramine composite (HMX/PU). Ritchie, Hsieh, and Kuo (1992) also found that as they added oxidizer to the freestream flow, XM39 propellant did ignite and the delay time decreased as the concentration of oxidizer was increased. They also observed two different ignition sites, as well as migration of the initially luminous region from the shoulder of the cylinder to the wake region which acts as a flameholder. Again, these results point to a requirement that the flow residence time must be greater than the characteristic time for the controlling gas-phase reaction (or system of reactions).

2.2 Aggregate (Packed Bed) Experiments. Possibly the earliest attempt to employ a *controlled* environment for studying convective ignition and flamespreading in a granular propellant bed is the work of Kuo et. al. during the mid-1970's (Kuo, Koo, Davis and Coates [1976]; Kuo and Koo [1977]). Because of the authors' interest in small-caliber ammunition (Olin WC-870 ball powder, 0.825-mm average diameter), the experiments were conducted in a heavy-wall steel tube with an inside diameter of only 7.77 mm (~0.3 in). The tube is divided into two sections by a nozzle plate (7 nozzles, each throat diameter = 1.59 mm [1/16 in]). The downstream section (length = 15.24 cm [6 in]) confines the ball powder sample, with a shear disc at the far end. The upstream section (4.76 cm [1.87 in]) contains the gas-phase ignition system — a hydrogen-oxygen mixture, initially sealed from the downstream section by some "tape" across the nozzle plate, is ignited by a spark plug. Ignition of the H_2/O_2 mixture drives a hot gas convective flame through the nozzle plate. Successful ignition of the granular propellant quickly pressurizes the downstream chamber, although the rate of pressurization is influenced by the "reverse" choked flow back into the igniter chamber. Data from the wall-mounted pressure transducers are used primarily to compare with numerical predictions from a two-phase flow model. The time-history from these transducers gives clear evidence of a steepening pressure front propagating through the chamber, which is an important result from this work. However, since all the data were generated from a single granular propellant, it is not possible to draw general conclusions about many aspects of convective ignition

Varney, Keeser, and Brandstadt (1979) developed a high-pressure flow-through (vented) chamber (2 in diameter, max length of 12 in) as part of an investigation of the "ignition effectiveness" which might be expected from several types of igniter materials. In Varney, Martino, and Henry (1983), this device was devoted to an ignition study of a Navy LOVA propellant; the data showed that successful ignition required significantly less igniter energy when the igniter flow contained oxidizer-rich species (from AP). This result was confirmed in a more comprehensive investigation by Varney, Martino, and Peters (1987) which employed a shortened (3.5 in length) version of the vented chamber device used earlier. Nine different constant-energy mixtures of igniter material (BP, NC, and blends of BP with AP, KP, AN, and KN) were evaluated as an ignition source for granular LOVA propellant (74.75% RDX, 12% CAB, 7.6% ATEC, 4% NC, 1.25% KS, 0.4% EC). Again, the oxidizer-rich igniter materials were found to significantly reduce the ignition delay time. Furthermore, LOVA ignition did not occur if the length of the bed was less than some minimum value (although the propellant grains would lose mass in a pyrolysis process). The authors also found that ignition delay time would increase if the igniter products "over-penetrated" the bed (i.e., they were driven into the bed at high velocity). These last two results strongly suggest a minimum residence time for the igniter gases in the aggregate of granular propellant.

Chang (1984) and Chang and Rocchio (1988) developed a laboratory device which simulates a 105-mm tank gun, including the bayonet primer along the centerline and intrusion of the projectile tail back into the chamber. Diagnostics include pressure time-history at several locations in addition to cinematography through the clear plastic walls which, of course, are sacrificed in a successful test. Granular propellants tested included M30 and four early LOVAs (CAB/NC/RDX). Chang (1984) found that the LOVA propellants were more difficult to ignite than M30 in the 105-mm simulator, and an igniter mixture 6828 ($NC/NG/KClO_4/EC$ :: 26/17/57/1) whose products included free oxygen would reduce the ignition delay time for the LOVA propellants by one half compared to a Benite igniter. However, the faster ignition with the 6828 igniter led to rapid flamespreading and the formation of pressure waves. Furthermore, changes to the configuration (hole sizes, etc.) of the bayonet primer had a significant influence on ignition delay times.

Messina, Ingram, and Tricarico (1988) built a special 25-mm-diameter transparent simulator to investigate the early-time events in a particular 25-mm APFSDS cartridge. This chamber incorporated the actual primer as well as the intrusion of the tail-boom assembly of the projectile. The authors found that, for XM39 LOVA propellant, the presence of ullage near the primer location led to long ignition delay times; however, the ignition delays nearly vanished when the ullage was placed at the forward end of the cartridge, and when the LOVA propellant was replaced by a high-energy, double-base propellant. These results would seem to indicate the presence of an important residence time as well as differences in the thermal threshold for convective ignition. In support of the Navy 76-mm/62 program, Messina, Ingram, and Konig (1989) developed a full-scale 76-mm ballistic simulator to investigate the ignition and flamespreading behavior in a granular Navy LOVA propellant during the evaluation of certain igniter compositions and geometric configurations. The benite igniter material, whose combustion products contain no free oxygen, was much less effective in igniting the LOVA propellant than LI-10 igniter material which produces 10 mole % of free oxygen. The authors also noted that approximately doubling the vent area in a primer tube with benite material caused a significant increase in ignition delay time.

3. FLAMESPREADING CHAMBER EXPERIMENT

The current experiment is not intended to simulate a particular primer, or to evaluate the performance of a class of igniter materials. The objective here is to study ignition and longitudinal flamespreading in a bed of granular gun propellant, particularly LOVA propellant. Within practical limitations, the desired experiment should have:

(a) an ignition source which will drive a planar wave through the chamber;
(b) an ignition wave composed of gas-phase products only;
(c) an ignition source which is reproducible but would permit the gas composition to be changed;
(d) and a chamber with closed volume.

Requirements (a) and (b) are intended to create an environment which is easy to model; for example, condensed-phase igniter products are known to be very effective in promoting ignition, but their behavior is difficult to represent in a theoretical model. Furthermore, a gas-phase-only ignition wave should directly influence the reactive gas phase in the granular bed which, based on data from previous convective ignition experiments, may be a controlling influence. The purpose of (d) is to simulate the gun combustion chamber which will trap and retain all pyrolysis products from the solid propellant. Finally, the ignition wave should have a rise time of 2–4 ms and maintain a pressure level within the range of 1–4 MPa for the purpose of recreating the marginal ignition environment suggested by the simulator experiments of Lang and Rocchio (1988).

Figure 1 is a schematic of the dual chamber apparatus designed to meet the above objectives. The operation is straightforward. A small quantity of ball powder is burned in the igniter chamber which is sealed by a diaphragm and a multiple-nozzle plate from the flow chamber which contains the sample granular material. When the diaphragm bursts, combustion gases initially confined in the igniter chamber are driven through the nozzle plate forming a planar wave of hot gases which propagates through the flow chamber. The rise time and strength of the ignition wave should be a function of the amount of ball powder burned in the igniter chamber, the burst pressure of the diaphragm covering the nozzle plate, the size of the nozzle holes, etc. Heat losses to the walls of the flow chamber will be minimized with the use of an acrylic liner (12.7-mm thick [0.5 in]) which also allows high-speed cinematography through window openings in the outer steel chamber. A blowout disc at the far end of the flow chamber should limit the maximum chamber pressure.

The inside diameter of the igniter chamber is 69.8 mm (2.75 in) and, in the present configuration, the length or height is 35 mm (1.375 in). However, various length internal sleeves can be used to adjust the height (hence, volume) as an additional control on the pressurization rate. A 12.7-mm (0.5 in) thick steel nozzle plate with 101 2.38-mm-diameter holes separates the igniter chamber from the flow chamber. The flow chamber contains a replaceable acrylic liner with an inside diameter of 76 mm (3 in) and a length of 304.8 mm (12 in). The dashed lines shown in Figure 1 indicate the window areas in the outer steel chamber which expose the acrylic liner (for photography). In the present configuration, four wall-mounted Kistler 211B1 pressure transducers provide a description of the chamber events; P_0 is in the igniter chamber, P_1 is 19 mm (0.75 in) into the flow chamber, P_2 is located at 120.6 mm (4.75 in), and P_3 is at 273 mm (10.75 in).

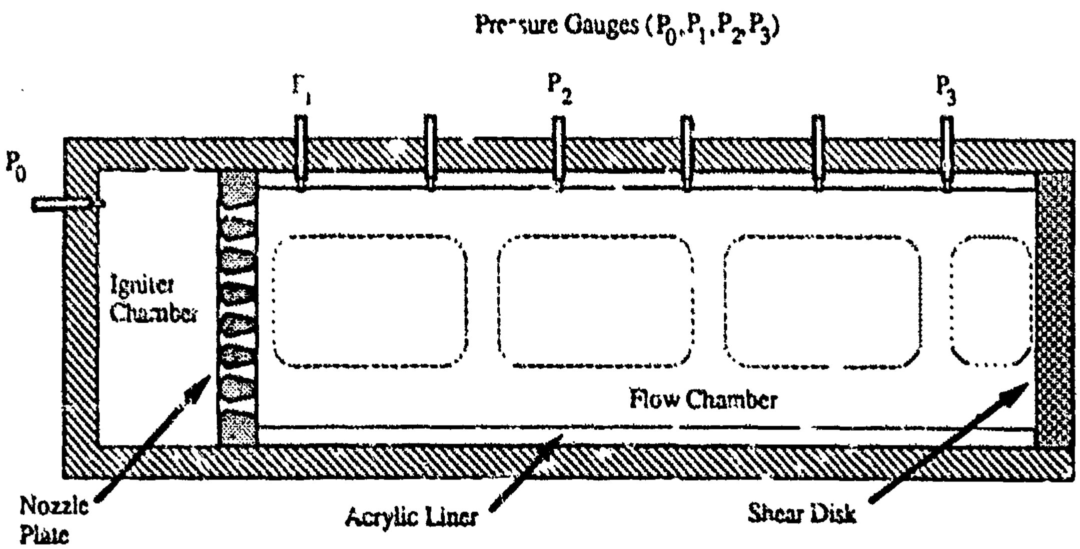

Figure 1. Schematic of flamespreading chamber apparatus.

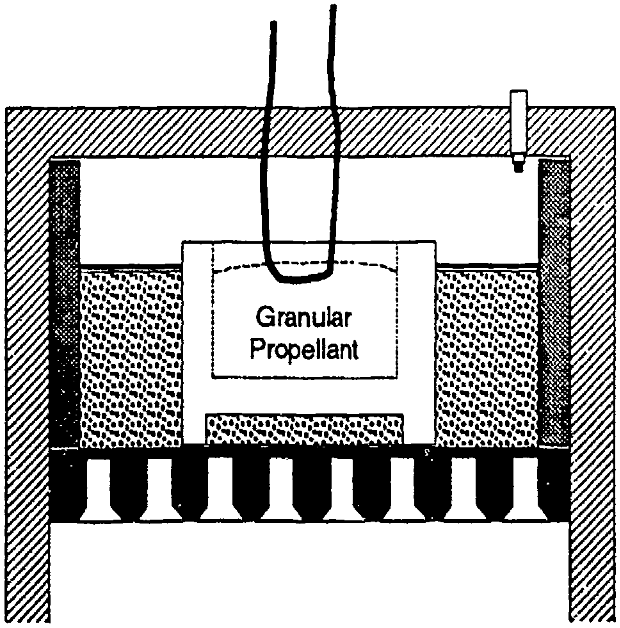

Figure 2. Schematic of igniter chamber/diaphragm system.

Design of the diaphragm covering the nozzle plate required some trial and error. The diaphragm must retain its integrity while pressure builds in the igniter chamber and combustion of the ball powder is well under way. It must then burst reliably to start the flow through the nozzle plate. An additional problem is to prevent the burning ball powder from being entrained into the flow through the nozzle plate and, hence, entering the flow chamber; this would create the unwanted two-phase ignition environment. Figure 2 is a schematic of the current system. Typically, 5 g of Olin ball powder (undeterred WC-870, average particle diameter of 0.775 mm) are placed within a 38-mm (1.5 in) diameter aluminum "cup" and then ignited near the top with a bridge wire; the cup is thermally insulated to minimize heat loss. The diaphragm system is multi-layered. Pressure sealing is done by two thicknesses of mylar which cover the nozzle plate. The other materials serve as a thermal shield to prevent hot ball powder particles from prematurely burning through the mylar discs before they reach their burst pressure. Two layers of aluminum foil in the shape of a donut (inside diameter = 50.8 mm) are placed directly on top of the mylar discs. Then the aluminum cup is surrounded by another donut (inside diameter = 38 mm) of "furnace filter" material approximately 18 mm in height; this donut of filter material is covered on the top by a single layer of aluminum foil. These thermal layers are designed to protect the mylar discs from hot particles which may escape over the side of the cup.

Unless otherwise stated, all results below apply to a flow chamber which is empty (contains gas only [i.e., no granular solids]). Figure 3a shows a pressure time-history from the flamespreading chamber apparatus when the mylar discs were not thermally protected; the system behavior is a total failure. Figure 3b shows a similar run using the above thermal protection system for the mylar discs; the dual chamber system has the desired behavior. Note that as the pressure in the flow chamber rises to that of the igniter chamber, the nozzle plate system unchokes, leaving a fairly uniform pressure level in the flow chamber for approximately 100 ms.

It is of interest to compare the pressure-time environment created by the present flamespreading chamber apparatus with that from the earlier experiments on convective ignition in a shock tube. The pressure records shown in Figure 3b from the three wall-mounted gauges in the flow chamber are redrawn in Figure 4a during the initial 25-ms time window after diaphragm burst. In this particular run, the flow chamber pressure rises within approximately 4 ms to a value near 2.75 MPa (400 psi), and then increases slowly by 10%. The shock-tube experiment of Birk and Caveny (1980) produces the pressure time-history shown in Figure 4b on the transverse cylinder; as might be anticipated, the rise time is faster (less than 2 ms), but after a few oscillations the pressure level becomes fairly uniform. A typical result from Ritchie, Hsieh, and Kuo (1990b) reproduced in Figure 4c also shows a rise time of 2 ms, a slight oscillation in pressure level, and then a 27% pressure rise over 16 ms, apparently caused by the addition of the upstream throat system in the shock tunnel. It appears that the present flamespreading chamber experiment is capable of generating a pressure environment which is similar to the shock tunnel, but with reduced harshness. The environment is also quite similar to that found by Chang and Rocchio (1988) during ignition anomalies in the 105-mm simulator. Figure 5 shows an example of the behavior when the flamespreading chamber is filled with inert granular propellant (diameter of 10 mm, length of 24 mm); the initial response of the three gauges suggest a wave propagating at approximately 220 m/s which is a typical value (see Kooker [1988]). The overshoot in Figure 5 reported by the farthest gauge (P_3, near the shear-disc) may have been the result of momentary bed motion caused by nonuniform packing. Several runs were conducted to check repeatability of this behavior; however, the igniter chamber suddenly developed a gas leak which then compromised these results. Reproducibility will be checked in future runs, once the gas leak has been repaired. Assuming it will be possible to control some of the smaller features of the pressure response curves, the flamespreading chamber should prove to be a useful tool in developing a database which may help explain convective ignition behavior in packed beds of granular propellant.

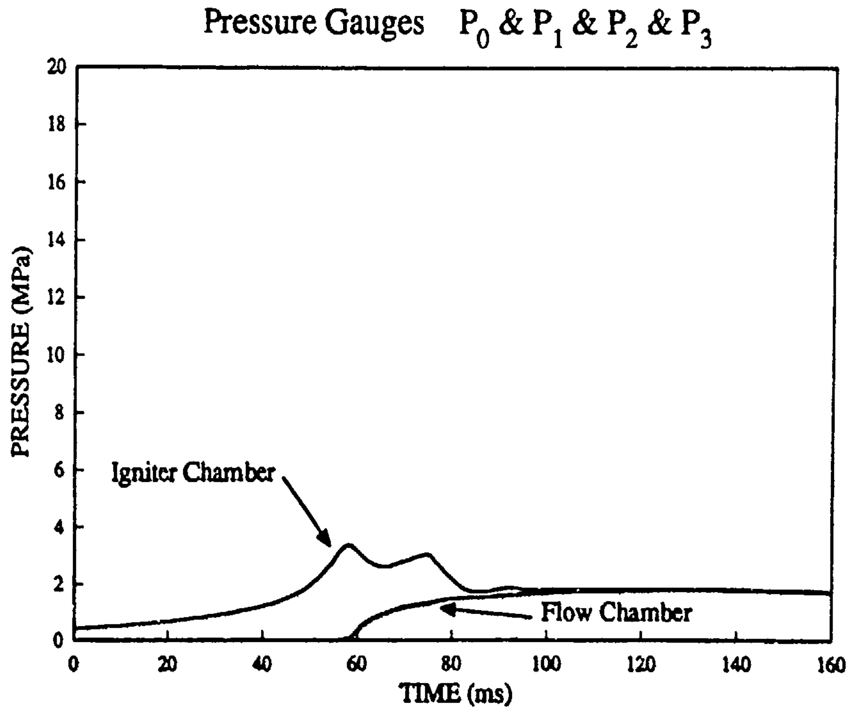

Figure 3a. Igniter chamber/flow chamber pressure time-history; diaphragm failure.

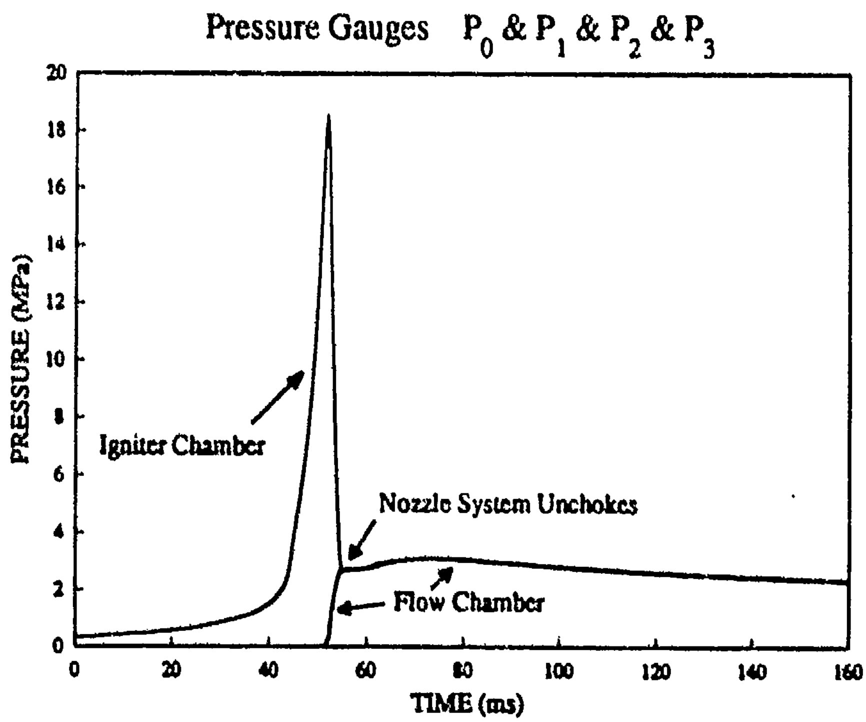

Figure 3b. Igniter chamber/flow chamber pressure time-history; successful diaphragm opening.

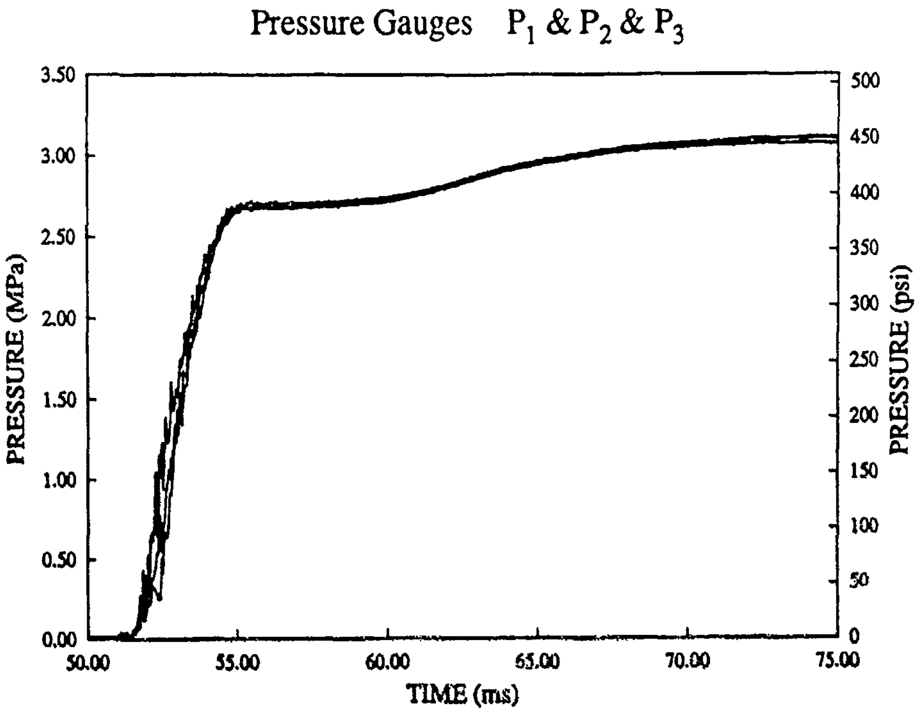

Figure 4a. Flow chamber pressure time-history from the 3 wall-mounted gauges (from Figure 3b); successful diaphragm opening.

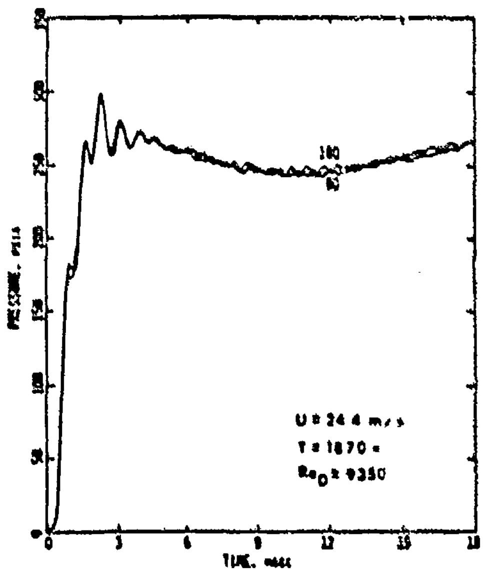

Figure 4b. Pressure time-history on cylinder in shock tunnel as measured by Birk and Caveny (1980).

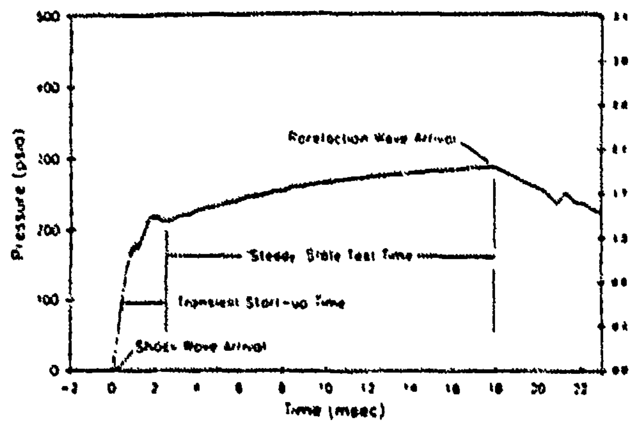

Figure 4c. Pressure time-history in modified shock tunnel as measured by Ritchie, Hsieh, and Kuo (1990).

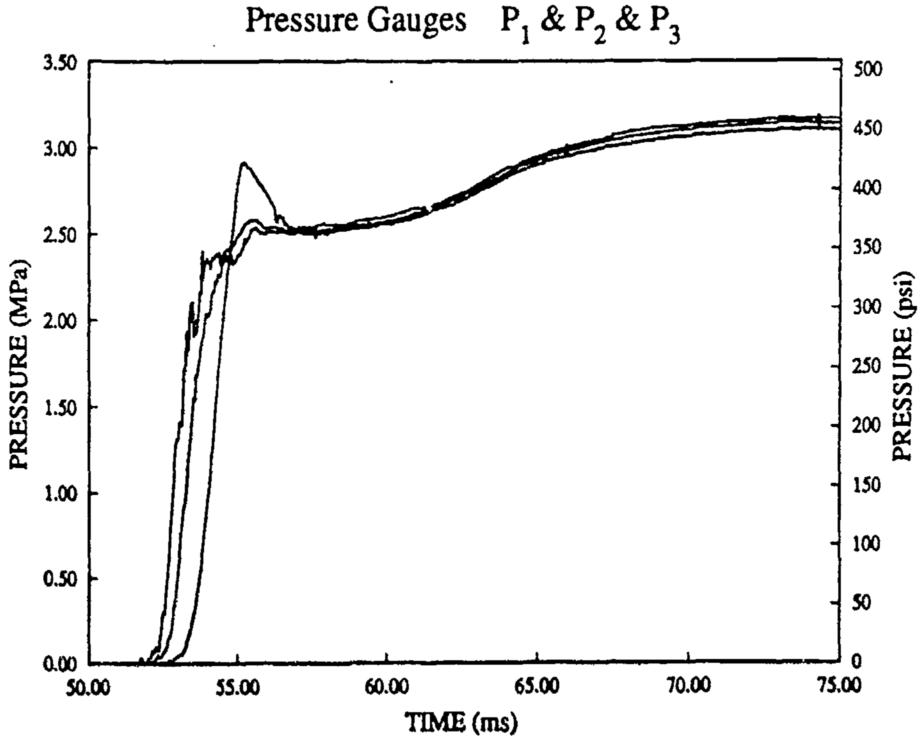

Figure 5. Flow chamber pressure time-history from the three wall-mounted gauges; flow chamber contains inert granular propellant.

4. MODEL OF THE FLAMESPREADING CHAMBER

A simple lumped-parameter model of the dual chamber system was constructed to predict the response to various parametric changes. The model encompasses both chambers illustrated in Figure 1. The analysis of the igniter chamber adopts the same well-stirred reactor equations derived for the closed-chamber burning rate reduction program "BRLCB" (Oberle and Kooker 1992). In the present version of the model, all combustion is assumed to take place in the igniter chamber. When the pre-set diaphragm burst pressure has been exceeded, the igniter chamber equations provide for a mass loss term which accounts for the flow through the nozzle plate system. Initially, a choked flow condition describes this mass flux which then "fills" the flow chamber. As the pressure in the flow chamber rises, the analysis senses the particular value at which the nozzle system unchokes. This normally provides a dramatic change in the rate of pressurization or depressurization of the system. The analysis accounts for convective heat transfer to the inside surface area of the multiple nozzles in the nozzle plate, but the flow chamber is assumed adiabatic because of the acrylic liner at the circumferential walls.

Model predictions of the igniter chamber pressure (e.g., Figure 6a) suggest several important characteristics of the diaphragm and nozzle plate system. Once the diaphragm rupture pressure has been exceeded, the dashed line in Figure 6a shows the expected depressurization of the igniter chamber for isentropic flow through the full geometric area of the nozzle plate. The chain-dash line is the expected depressurization curve if the *effective* nozzle area (A_{en}) were only 40% of the geometric area (as a result of all flow losses). The solid line, in addition, assumes that the diaphragm rupture process occurs in a finite time interval; it is assumed here that the nozzle area opens linearly in a 1-ms time interval. This last curve more nearly approximates the actual behavior of the apparatus. Figure 6b shows typical behavior for both chambers—the solid line is the igniter chamber and the chain-dash line is the flow chamber. Unchoking of the converging/diverging nozzle system occurs as the pressures are nearly equal (just after 10 ms, here). The dashed curve represents grams of igniter propellant remaining to be consumed (although the label on the scale says MPa). (Note that at unchoking, approximately 1.5 g of the original 5 g remains to burn.) This plays a role in controlling the increase or decrease of the flow chamber pressure as a function of time. The model suggests two other ways to modify the pressure time curve in the flow chamber. Figure 7a shows the predicted effect of raising the diaphragm burst pressure from 10 to 20 MPa, while burning 5 g of ball powder in the igniter chamber. Figure 7b shows that a possible mechanism to compensate for heat losses is a slight increase in the mass of ball powder burned in the igniter chamber while keeping the diaphragm burst pressure constant (15 MPa, here).

Figure 8 shows a plot of pressure time-histories (Run #14) from the four gauges along with model predictions which assume a burst pressure of 14 MPa, 1.5-ms diaphragm opening time, and 40% effective flow area of the 4.5-cm^2 nozzle plate. Before the time of diaphragm burst, the comparison with igniter chamber pressure in Figure 8a is not particularly good; note, however, the model assumes that all the ball powder grains are ignited at time zero, while the experiment ignites the ball powder from the top with a bridge wire. After diaphragm burst, however, the comparison is fairly good, including the prediction of the pressure level at which the nozzle system unchokes. Figure 8b compares the flow chamber pressure time-history (at gauge P_1) with two theoretical predictions; the chain-dash curve assumes maximum heat loss to the steel nozzle walls (isothermal walls) and the dashed curve assumes no heat loss (adiabatic wall). The comparison shows that the isothermal curve characterizes the rise time and plateau level up to approximately 16 ms, but then the curve turns up in the direction of the adiabatic prediction. This is typical of the comparisons; after the plateau value, the rising level of flow chamber pressure seems to indicate a saturation of the heat transfer to the nozzle walls (i.e., the surface temperature of the nozzle walls may momentarily approach that of the gas flow). However, not all comparisons show this degree of agreement Figure 9 displays the results from Run #31. The prediction of the unchoking value of

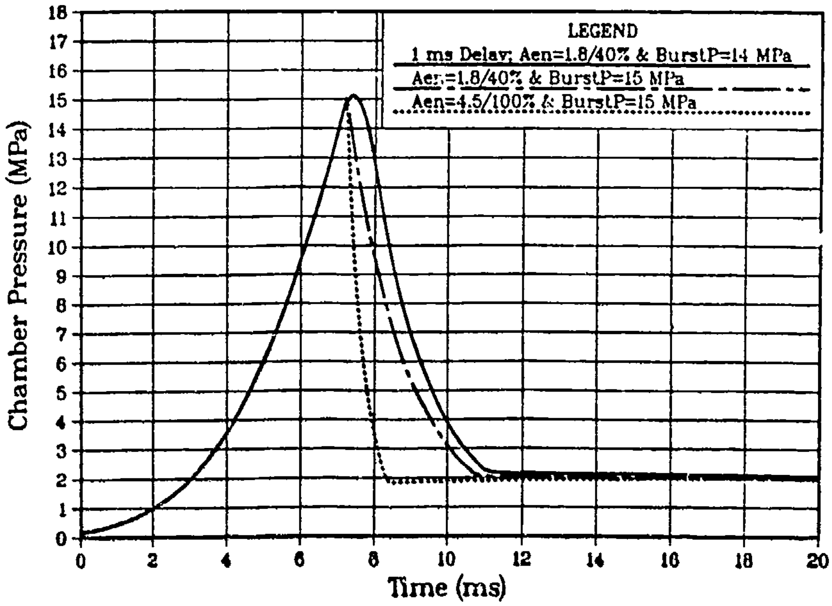

Figure 6a. Model predictions for flamespreading chamber: igniter chamber pressure time-history [dash = isentropic flow through 100% of nozzle area, chain-dash = isentropic flow through 40% of nozzle area, solid = 1 ms delay opening of 40% nozzle area (A_{en} in cm^2 here)].

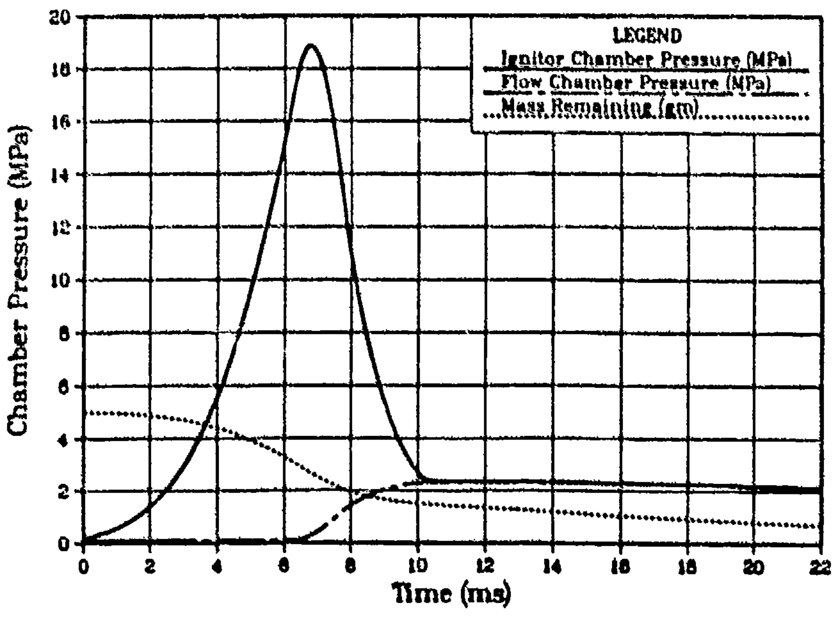

Figure 6b. Model predictions for flamespreading chamber: typical pressure time-history [solid = igniter chamber, chain-dash = flow chamber, dash = mass of ball powder remaining in igniter chamber] Note: mass remaining (gm) is plotted on same scale as chamber pressure.

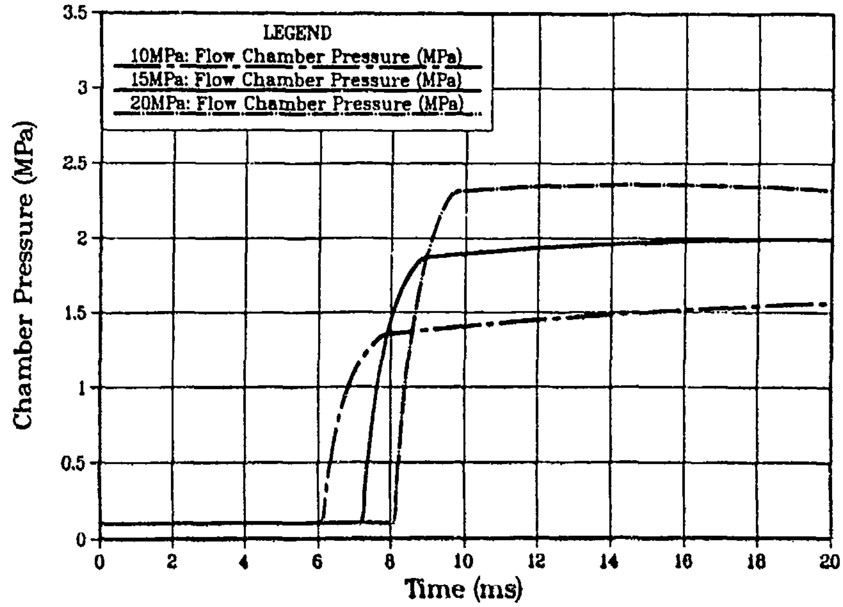

Figure 7a. Model predictions for flow chamber pressure time-history. Combustion of 5-g ball powder in igniter chamber. Influence of diaphragm burst pressure: chain-dash = 10 MPa, solid = 15 MPa, chain-dot = 20 MPa. Calculation assumes zero time delay in nozzle opening.

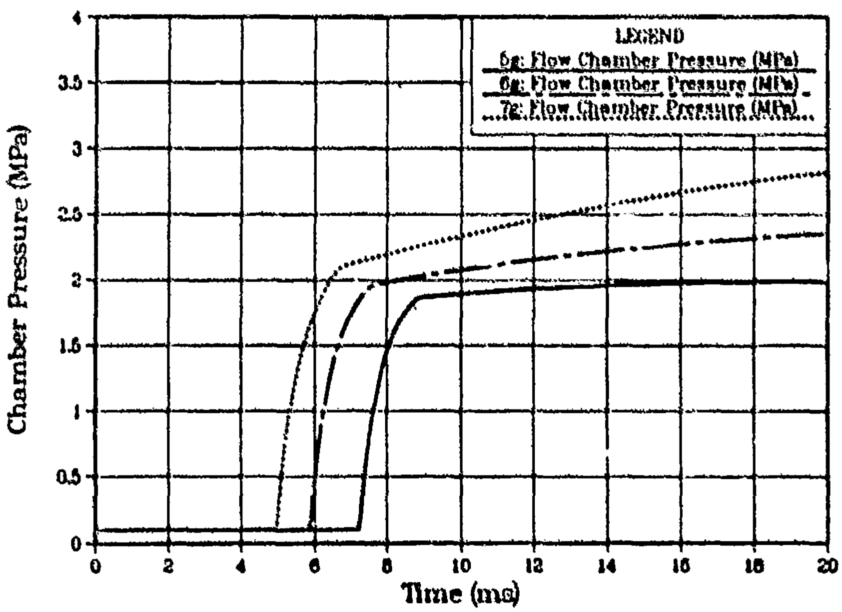

Figure 7b. Model predictions for flow chamber pressure time-history. Diaphragm burst pressure is 15 MPa. Influence of mass of ball powder burned in igniter chamber: solid = 5 g, chain-dash = 6 g, dot = 7 g. Calculation assumes zero time delay in nozzle opening.

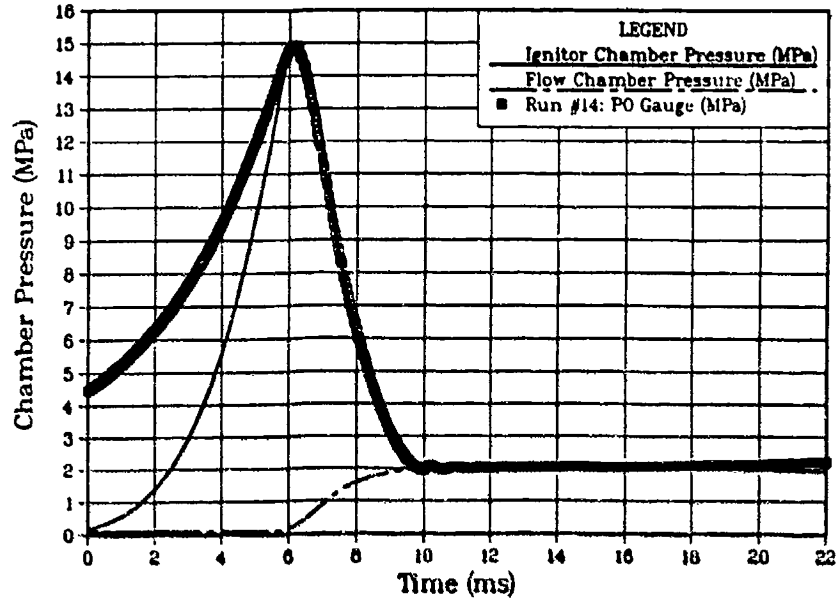

Figure 8a. Comparison of model predictions/data from run #14: pressure time-history in igniter chamber. Burst pressure = 13 MPa, 1.5 ms delayed opening of 40% nozzle area (solid = igniter chamber, chain-dash = flow chamber).

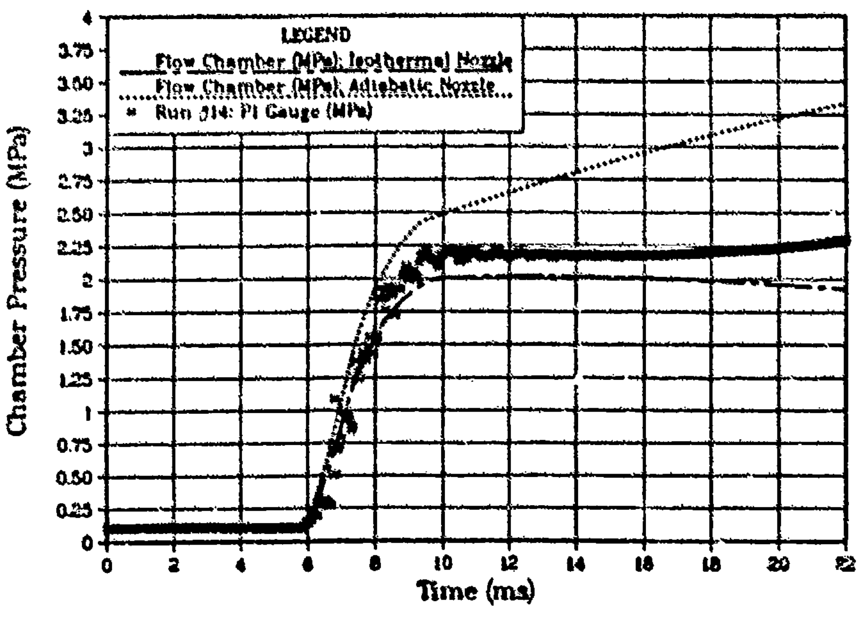

Figure 8b. Comparison of model predictions/data from run #14: pressure time-history in flow chamber (no granular solids). Burst pressure = 13 MPa, 1.5 ms delayed opening of 40% nozzle area (chain-dash => isothermal nozzle, dash => adiabatic nozzle).

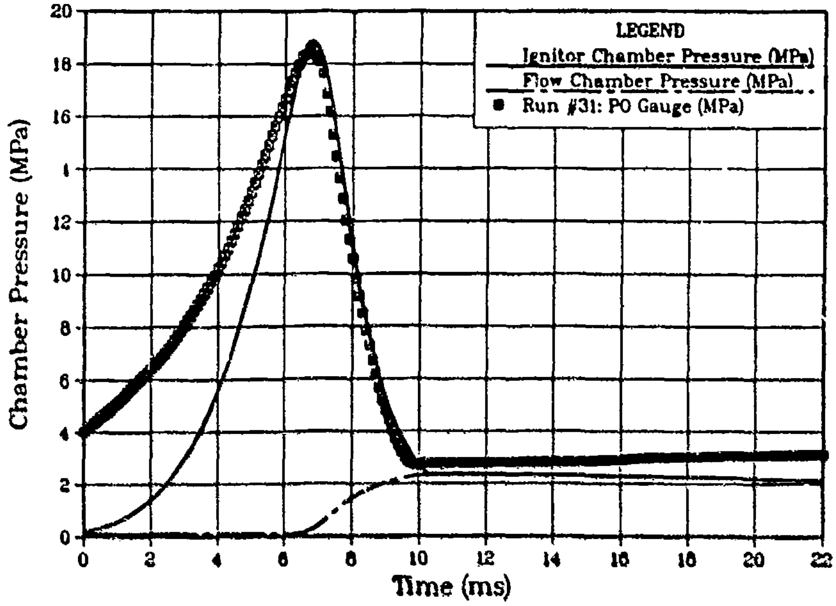

Figure 9a. Comparison of model predictions/data from run #31: pressure time-history in igniter chamber. Burst pressure = 17 MPa, 1.5 ms delayed opening of 40% nozzle area (solid = igniter chamber, chain-dash = flow chamber).

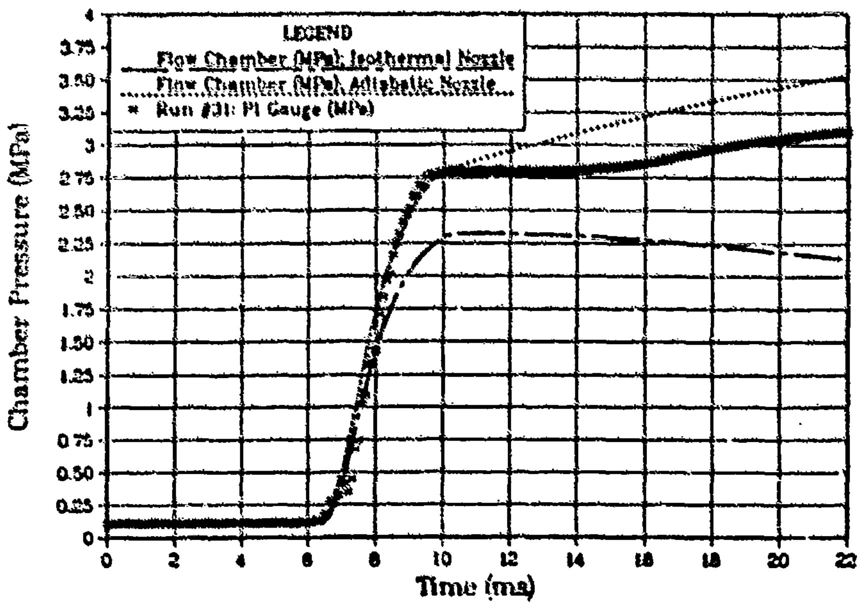

Figure 9b. Comparison of model predictions/data from run #31: pressure time-history in flow chamber (no granular solids). Burst pressure = 17 MPa, 1.5 ms delayed opening of 40% nozzle area (chain-dash => isothermal nozzle, dash => adiabatic nozzle).

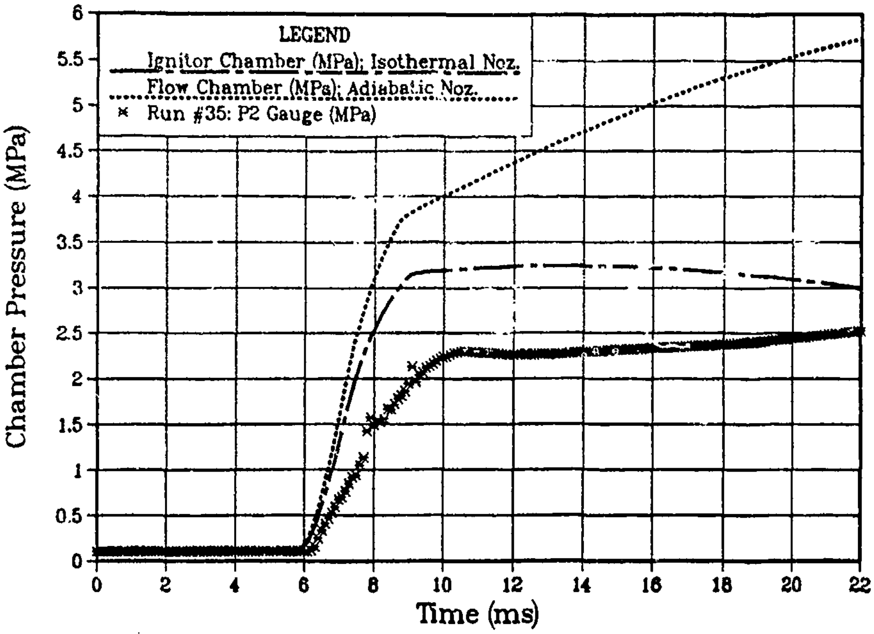

Figure 10. Comparison of model predictions/data from run #35: pressure time-history in flow chamber (WITH inert granular solids). Burst pressure = 17.5 MPa, flow chamber volume = 800 cm^3 (chain-dash => isothermal nozzle, dash => adiabatic nozzle).

pressure is not quite as accurate, as seen in Figure 9a. The measured flow chamber pressure (again, gauge P_1) shown in Figure 9b suggests that the initial pressure rise follows the adiabatic approximation rather than the isothermal, which is contrary to intuition. There still may be some subtleties which the model has neglected.

Finally, Figure 10 shows a comparison of the flow chamber pressure (gauge P_2) for a case when the chamber was filled with inert granular propellant. To account for the presence of the solid phase, the flow chamber volume available for the gas phase was appropriately reduced in this model prediction. However, the model ignores heat loss from the hot gas to the solid grains, which judging from the comparison with the experimental data, is substantial. The model will be upgraded in the near future to account for both phases in the flow chamber.

5. CONCLUDING REMARKS

The current flamespreading chamber design appears to create a planar gas-phase ignition wave which will propagate from one end of a flow chamber through the confined sample granular material. With the proper thermal protection for the diaphragm material which seals the nozzle plate, the apparatus generates a pressure wave with a rise time of approximately 3 ms to a range of pressures between 1–4 MPa for a time interval of at least 50 ms. This should provide enough flexibility to create an environment for studying the marginal convective ignition behavior of many compositions of granular solid propellant, especially LOVA propellants. The current lumped-parameter model of the dual chamber apparatus has been helpful in interpreting several features of the pressure response curves.

Future work will include an attempt to use shielded thermocouples to measure gas-phase temperature within the compacted aggregate of granular propellant. Simultaneous data for static pressure and temperature in the gas phase should help define the convective environment imposed on the granular propellant bed. It is hoped that data from this flamespreading chamber will prove particularly valuable in validating predictions of gun propellant ignition within interior ballistic models.

6. REFERENCES

Birk, A., and L. H. Caveny. "Convective Ignition of Propellant Cylinders in a Developing Cross-Flow Field." MAE Report 1486, Department of Mechanical and Aerospace Engineering, Princeton University, Princeton, NJ, September 1980a.

Birk, A., and L. H. Caveny. "Convective Ignition of Propellant Cylinders in a Developing Flowfield." AIAA Journal, vol. 18, no. 11, pp. 1363–1403, November 1980b.

Chang, L-M. "Early Phase Ignition Phenomena Observed in a 105 mm Tank Gun Chamber." 21st JANNAF Combustion Meeting, CPIA Publication 412, vol. II, pp. 301–311, October 1984.

Chang, L-M., and J. J. Rocchio. "Simulator Diagnostics of the Early Phase Ignition Phenomena in a 105-mm Tank Gun Chamber." BRL-TR-2890, U.S. Army Ballistic Research Laboratory, Aberdeen Proving Ground, MD, March 1988.

Horst, A. W. "Multiphase Flow Analysis of the Ballistic Performance of an Anomalous LOVA Propellant Mix." 20th JANNAF Combustion Meeting, CPIA Publication 383, vol. I, pp. 557-570, October 1983.

Kooker, D. E. "A Reactive Shock Wave Model for Compaction Waves in Granular Energetic Material." BRL-TR-2945, U.S. Army Ballistic Research Laboratory, Aberdeen Proving Ground, MD, November 1988.

Kuo, K. K., J. H. Koo, T. R. Davis, and G. R. Coates. "Transient Combustion in Mobile Gas-Permeable Propellants." Acta Astronautica, vol. 3, pp. 573—591, 1976.

Kuo, K. K. and J. H. Koo. "Transient Combustion in Granular Propellant Beds. Part I: Theoretical Modeling and Numerical Solution of Transient Combustion Processes in Mobile Granular Propellant Beds." Contract Report 346, U. S. Army Ballistic Research Laboratory, Aberdeen Proving Ground, MD, August 1977.

Messina, N. A., L. S. Ingram, and G. F. Konig. "A 76 mm Ballistic Simulator for the Diagnostic Evaluation of Ignition, Flamespreading, and Combustion Behavior." 26th JANNAF Combustion Meeting, CPIA Publication 529, vol. III, pp. 145–164, October 1989.

Messina, N. A., L. S. Ingram, S. O. Morris, and K. Rice. "A Ballistic Simulator for the Diagnostic Evaluation of the Start-up Transient in 76 mm Ammunition." Collected viewgraphs in A Review of Recent Work in the Area of LOVA Gun Propellant Ignition, CPIA 576, pp. 117–132, August 1991.

Messina, N. A., L. S. Ingram, and S. A. Tricarico. "25 mm Ballistic Simulator for XM919 Ignition System/Charge Design Optimization." 25th JANNAF Combustion Meeting, CPIA Publication 498, vol. IV, pp. 379–396, October 1988.

Miller, M. S. "Modeling of Kinetics and Combustion of Energetic Materials." ARO-URI Meeting on Fast Reaction Kinetics and Modeling of Energetic Material Combustion, The Pennsylvania State University, 6–7 August 1992.

Oberle, W., and D. E. Kooker. "BRLCB: A Closed-Chamber Data Analysis Program - Theory and User's Manual (Parts I and II)." ARL-TR-36, U. S. Army Research Laboratory, Aberdeen Proving Ground, MD, January 1993; also see "Modifications and Updates to the Closed-Chamber Data Analysis Program BRLCB, Including Provisions for ETC Propellant Analysis." 29th JANNAF Combustion Meeting, NASA/Langley, Hampton VA, 19–22 October 1992.

Ritchie, S. J., W-H. Hsieh, and K. K. Kuo. "Convective Ignition of LOVA Propellants Subjected to Crossflow Heating Conditions." 26th JANNAF Combustion Meeting, CPIA Publication 529, vol. I, pp. 1–12, October 1989.

Ritchie, S. J., W-H. Hsieh, and K. K. Kuo "Convective Ignition Phenomena of LOVA Propellants." AIAA Paper 90-2194, 26th AIAA/SAE/ASME/ASEE Joint Propulsion Conference, 16–18 July 1990a.

Ritchie, S. J., W-H. Hsieh, and K. K. Kuo. "Convective Ignition of LOVA Propellants." 27th JANNAF Combustion Meeting, CPIA Publication 557, vol. I, pp. 287–298, November 1990b.

Ritchie, S. J., W-H. Hsieh, and K. K. Kuo. "Ignition of RDX-Based Solid Propellant Subjected to Crossflow Convective Heating." AIAA Journal of Propulsion and Power, vol. 8, no. 3, pp. 570–577, May–June 1992.

Varney, A. M., J. W. Keeser, and R. Brandstadt. "An Ignition Energetics Characterization Device for Porous Bed Gun Propellants." 16th JANNAF Combustion Meeting, CPIA Publication 308, vol. I, pp. 653–672, September 1979.

Varney, A. M., J. Martino, and R. Henry. "Ignitibility Studies of LOVA Propellants." 20th JANNAF Combustion Meeting, CPIA Publication 383, vol. I, pp. 547–556, October 1983.

Varney, A. M., J. Martino, and S. Peters. "Enhancement Techniques for Igniting LOVA Propellants." 24th JANNAF Combustion Meeting, CPIA Publication 476, vol. III, pp. 235–249, October 1987.

No. of Copies	Organization
2	Administrator Defense Technical Info Center ATTN: DTIC-DDA Cameron Station Alexandria, VA 22304-6145
1	Commander U.S. Army Materiel Command ATTN: AMCAM 5001 Eisenhower Ave. Alexandria, VA 22333-0001
1	Director U.S. Army Research Laboratory ATTN: AMSRL-OP-CI-AD, Tech Publishing 2800 Powder Mill Rd. Adelphi, MD 20783-1145
1	Director U.S. Army Research Laboratory ATTN: AMSRL-OP-CI-AD, Records Management 2800 Powder Mill Rd. Adelphi, MD 20783-1145
2	Commander U.S. Army Armament Research, Development, and Engineering Center ATTN: SMCAR-IMI-I Picatinny Arsenal, NJ 07806-5000
2	Commander U.S. Army Armament Research, Development, and Engineering Center ATTN: SMCAR-TDC Picatinny Arsenal, NJ 07806-5000
1	Director Benet Weapons Laboratory U.S. Army Armament Research, Development, and Engineering Center ATTN: SMCAR-CCB-TL Watervliet, NY 12189-4050
(Unclass. only) 1	Commander U.S. Army Rock Island Arsenal ATTN: SMCRI-IMC-RT/Technical Library Rock Island, IL 61299-5000
1	Director U.S. Army Aviation Research and Technology Activity ATTN: SAVRT-R (Library) M/S 219-3 Ames Research Center Moffett Field, CA 94035-1000

No. of Copies	Organization
1	Commander U.S. Army Missile Command ATTN: AMSMI-RD-CS-R (DOC) Redstone Arsenal, AL 35898-5010
1	Commander U.S. Army Tank-Automotive Command ATTN: ASQNC-TAC-DIT (Technical Information Center) Warren, MI 48397-5000
1	Director U.S. Army TRADOC Analysis Command ATTN: ATRC-WSR White Sands Missile Range, NM 88002-5502
1	Commandant U.S. Army Field Artillery School ATTN: ATSF-CSI Ft. Sill, OK 73503-5000
(Class. only) 1	Commandant U.S. Army Infantry School ATTN: ATSH-CD (Security Mgr.) Fort Benning, GA 31905-5660
(Unclass. only) 1	Commandant U.S. Army Infantry School ATTN: ATSH-CD-CSO-OR Fort Benning, GA 31905-5660
1	WL/MNOI Eglin AFB, FL 32542-5000

Aberdeen Proving Ground

No. of Copies	Organization
2	Dir, USAMSAA ATTN: AMXSY-D AMXSY-MP, H. Cohen
1	Cdr, USATECOM ATTN: AMSTE-TC
1	Dir, ERDEC ATTN: SCBRD-RT
1	Cdr, CBDA ATTN: AMSCB-CI
1	Dir, USARL ATTN: AMSRL-SL-I
10	Dir, USARL ATTN: AMSRL-OP-CI-B (Tech Lib)

No. of Copies	Organization
1	Chairman DOD Explosives Safety Board Room 856-C Hoffman Bldg. 1 2461 Eisenhower Avenue Alexandria, VA 22331-0600
1	Headquarters U.S. Army Materiel Command ATTN: AMCICP-AD, M. Fisette 5001 Eisenhower Ave. Alexandria, VA 22333-0001
1	U.S. Army Ballistic Missile Defense Systems Command Advanced Technology Center P.O. Box 1500 Huntsville, AL 35807-3801
1	Department of the Army Office of the Product Manager 155mm Howitzer, M109A6, Paladin ATTN: SFAE-AR-HIP-IP, Mr. R. De Kleine Picatinny Arsenal, NJ 07806-5000
3	Project Manager Advanced Field Artillery System ATTN: SFAE-ASM-AF-E, LTC D. Ellis T. Kuriata J. Shields Picatinny Arsenal, NJ 07801-5000
1	Project Manager Advanced Field Artillery System ATTN: SFAE-ASM-AF-Q, W. Warren Picatinny Arsenal, NJ 07801-5000
2	Commander Production Base Modernization Agency U.S. Army Armament Research, Development, and Engineering Center ATTN: AMSMC-PBM, A. Siklosi AMSMC-PBM-E, L. Laibson Picatinny Arsenal, NJ 07806-5000

No. of Copies	Organization
4	PEO-Armaments Project Manager Tank Main Armament System ATTN: AMCPM-TMA AMCPM-TMA-105 AMCPM-TMA-120 AMCPM-TMA-AS, H. Yuen Picatinny Arsenal, NJ 07806-5000
4	Commander U.S. Army Armament Research, Development, and Engineering Center ATTN: SMCAR-CCH-V, C. Mandala E. Fennell SMCAR-CCH-T, L. Rosendorf SMCAR-CCS Picatinny Arsenal, NJ 07806-5000
19	Commander U.S. Army Armament Research, Development, and Engineering Center ATTN: SMCAR-AEE, J. Lannon SMCAR-AEE-B, A. Beardell D. Downs S. Einstein S. Westley S. Bernstein J. Rutkowski B. Brodman P. O'Reilly R. Cirincione A. Grabowsky P. Hui J. O'Reilly SMCAR-AEE-WW, M. Mezger J. Pinto D. Wiegand P. Lu C. Hu SMCAR-AES, S. Kaplowitz Picatinny Arsenal, NJ 07806-5000
1	Commander U.S. Army Armament Research, Development and Engineering Center ATTN: SMCAR-HFM, E. Barrieres Picatinny Arsenal, NJ 07806-5000

No. of Copies	Organization
9	Commander U.S. Army Armament Research, Development and Engineering Center ATTN: SMCAR-FSA-T, M. Salsbury SMCAR-FSA-F, LTC R. Riddle SMCAR-FSC, G. Ferdinand SMCAR-FS, T. Gora SMCAR-FS-DH, J. Feneck SMCAR-FSS-A, R. Kopman B. Machek L. Pinder SMCAR-FSN-N, K. Chung Picatinny Arsenal, NJ 07806-5000
3	Director Benet Weapons Laboratories ATTN: SMCAR-CCB-RA, G.P. O'Hara G.A. Pflegl SMCAR-CCB-S, F. Heiser Watervliet, NY 12189-4050
2	Commander U.S. Army Research Office ATTN: Technical Library D. Mann P.O. Box 12211 Research Triangle Park, NC 27709-2211
1	Commander, USACECOM R&D Technical Library ATTN: ASQNC-ELC-IS-L-R, Myer Center Fort Monmouth, NJ 07703-5301
1	Director U.S. Army Research Laboratory ATTN: AMSRL-D 2800 Powder Mill Rd. Adelphi, MD 20783-1145
1	Commandant U.S. Army Aviation School ATTN: Aviation Agency Fort Rucker, AL 36360
1	Program Manager U.S. Tank-Automotive Command ATTN: AMCPM-ABMS, T. Dean Warren, MI 48092-2498

No. of Copies	Organization
1	Project Manager U.S. Tank-Automotive Command Fighting Vehicle Systems ATTN: SFAE-ASM-BV Warren, MI 48397-5000
1	Project Manager, Abrams Tank System ATTN: SFAE-ASM-AB Warren, MI 48397-5000
1	Director HQ, TRAC RPD ATTN: ATCD-MA Fort Monroe, VA 23651-5143
1	Commander U.S. Army Belvoir Research and Development Center ATTN: STRBE-WC Fort Belvoir, VA 22060-5006
1	Director U.S. Army TRAC-Ft. Lee ATTN: ATRC-L, Mr. Cameron Fort Lee, VA 23801-6140
1	Commandant U.S. Army Command and General Staff College Fort Leavenworth, KS 66027
1	Commandant U.S. Army Special Warfare School ATTN: Rev and Trng Lit Div Fort Bragg, NC 28307
1	Commander Radford Army Ammunition Plant ATTN: SMCAR-QA/HI LIB Radford, VA 24141-0298
1	Commander U.S. Army Foreign Science and Technology Center ATTN: AMXST-MC-3 220 Seventh Street, NE Charlottesville, VA 22901-5396

No. of Copies	Organization
2	Commandant U.S. Army Field Artillery Center and School ATTN: ATSF-CO-MW, E. Dublisky ATSF-CN, P. Gross Ft. Sill, OK 73503-5600
1	Commandant U.S. Army Armor School ATTN: ATZK-CD-MS, M. Falkovitch Armor Agency Fort Knox, KY 40121-5215
1	U.S. Army European Research Office ATTN: Dr. Roy E. Richenbach Box 65 FPO New York 09510-1500
2	Commander Naval Sea Systems Command ATTN: SEA 62R SEA 64 Washington, DC 20362-5101
1	Commander Naval Air Systems Command ATTN: AIR-954-Tech Library Washington, DC 20360
4	Commander Naval Research Laboratory ATTN: Technical Library Code 4410, K. Kailasanate J. Boris E. Oran Washington, DC 20375-5000
1	Office of Naval Research ATTN: Code 473, R.S. Miller 800 N. Quincy Street Arlington, VA 22217-9999
1	Office of Naval Technology ATTN: ONT-213, D. Siegel 800 N. Quincy St. Arlington, VA 22217-5000

No. of Copies	Organization
3	Commander Naval Surface Warfare Center ATTN: Code 730 Code R-13, R. Bernecker H. Sandusky Silver Spring, MD 20903-5000
7	Commander Naval Surface Warfare Center ATTN: T.C. Smith K. Rice S. Mitchell S. Peters J. Consaga C. Gotzmer Technical Library Indian Head, MD 20640-5000
4	Commander Naval Surface Warfare Center ATTN: Code G30, Guns & Munitions Div Code G32, Guns Systems Div Code G33, T. Doran Code E23 Technical Library Dahlgren, VA 22448-5000
5	Commander Naval Air Warfare Center ATTN: Code 388, C.F. Price T. Boggs Code 3895, T. Parr R. Derr Information Science Division China Lake, CA 93555-6001
1	Commanding Officer Naval Underwater Systems Center ATTN: Code 5B331, Technical Library Newport, RI 02840
1	AFOSR/NA ATTN: J. Tishkoff Bolling AFB, D.C. 20332-6448
1	OLAC PL/TSTL ATTN: D. Shiplett Edwards AFB, CA 93523-5000

No. of Copies	Organization
3	AL/LSCF ATTN: J. Levine L. Quinn T. Edwards Edwards AFB, CA 93523-5000
1	WL/MNAA ATTN: B. Simpson Eglin AFB, FL 32542-5434
1	WL/MNME Energetic Materials Branch 2306 Perimeter Rd. STE 9 Eglin AFB, FL 32542-5910
1	WL/MNSH ATTN: R. Drabczuk Eglin AFB, FL 32542-5434
2	NASA Langley Research Center ATTN: M.S. 408, W. Scallion D. Witcofski Hampton, VA 23605
1	Central Intelligence Agency Office of the Central References Dissemination Branch Room GE-47, HQS Washington, DC 20502
1	Central Intelligence Agency ATTN: J. Backofen NHB, Room 5N01 Washington, DC 20505
1	SDIO/TNI ATTN: L.H. Caveny Pentagon Washington, DC 20301-7100
1	SDIO/DA ATTN: E. Gerry Pentagon Washington, DC 21301-7100
2	HQ DNA ATTN: D. Lewis A. Fahey 6801 Telegraph Rd. Alexandria, VA 22310-3398

No. of Copies	Organization
1	Director Sandia National Laboratories Energetic Materials & Fluid Mechanics Department, 1512 ATTN: M. Baer P.O. Box 5800 Albuquerque, NM 87185
1	Director Sandia National Laboratories Combustion Research Facility ATTN: R. Carling Livermore, CA 94551-0469
4	Director Lawrence Livermore National Laboratory ATTN: L-355, A. Buckingham G. Benedetti M. Finger L-324, M. Constantino P.O. Box 808 Livermore, CA 94550-0622
2	Director Los Alamos Scientific Lab ATTN: T3/D. Butler M. Division/B. Craig P.O. Box 1663 Los Alamos, NM 87544
2	Battelle ATTN: TACTEC Library, J.N. Huggins V. Levin 505 King Avenue Columbus, OH 43201-2693
1	Battelle PNL ATTN: Mr. Mark Garnich P.O. Box 999 Richland, WA 99352
1	Institute of Gas Technology ATTN: D. Gidaspow 3424 S. State Street Chicago, IL 60616-3896
1	Institute for Advanced Technology ATTN: T.M. Kiehne The University of Texas of Austin 4030-2 W. Braker Lane Austin, TX 78759-5329

No. of Copies	Organization
2	CPIA - JHU ATTN: H. J. Hoffman T. Christian 10630 Little Patuxent Parkway Suite 202 Columbia, MD 21044-3200
1	Brigham Young University Department of Chemical Engineering ATTN: M. Beckstead Provo, UT 84601
1	Jet Propulsion Laboratory California Institute of Technology ATTN: L.D. Strand, MS 125/224 4800 Oak Grove Drive Pasadena, CA 91109
1	California Institute of Technology 204 Karman Lab Main Stop 301-46 ATTN: F.E.C. Culick 1201 E. California Street Pasadena, CA 91109
3	Georgia Institute of Technology School of Aerospace Engineering ATTN: B.T. Zim E. Price W.C. Strahle Atlanta, GA 30332
1	Massachusetts Institute of Technology Department of Mechanical Engineering ATTN: T. Toong 77 Massachusetts Avenue Cambridge, MA 02139-4307
2	University of Illinois Department of Mechanical/Industry Engineering ATTN: H. Krier R. Beddini 144 MEB; 1206 N. Green St. Urbana, IL 61801-2978
1	University of Maryland ATTN: Dr. J.D. Anderson College Park, MD 20740

No. of Copies	Organization
1	University of Massachusetts Department of Mechanical Engineering ATTN: K. Jakus Amherst, MA 01002-0014
1	University of Minnesota Department of Mechanical Engineering ATTN: E. Fletcher Minneapolis, MN 55414-3368
3	Pennsylvania State University Department of Mechanical Engineering ATTN: V. Yang K. Kuo C. Merkle University Park, PA 16802-7501
1	Rensselaer Polytechnic Institute Department of Mathematics Troy, NY 12181
1	Stevens Institute of Technology Davidson Laboratory ATTN: R. McAlevy III Castle Point Station Hoboken, NJ 07030-5907
1	Rutgers University Department of Mechanical and Aerospace Engineering ATTN: S. Temkin University Heights Campus New Brunswick, NJ 08903
1	University of Southern California Mechanical Engineering Department ATTN: 0HE200, M. Gerstein Los Angeles, CA 90089-5199
1	University of Utah Department of Chemical Engineering ATTN: A. Baer Salt Lake City, UT 84112-1194
1	Washington State University Department of Mechanical Engineering ATTN: C.T. Crowe Pullman, WA 99163-5201

No. of Copies	Organization
1	AFELM, The Rand Corporation ATTN: Library D 1700 Main Street Santa Monica, CA 90401-3297
1	Arrow Technology Associates, Inc. ATTN: W. Hathaway P.O. Box 4218 South Burlington, VT 05401-0042
3	AAI Corporation ATTN: J. Hebert J. Frankle D. Cleveland P.O. Box 126 Hunt Valley, MD 21030-0126
2	Alliant Techsystems, Inc. ATTN: R.E. Tompkins J. Kennedy 7225 Northland Dr. Brooklyn Park, MN 55428
1	AVCO Everett Research Laboratory ATTN: D. Stickler 2385 Revere Beach Parkway Everett, MA 02149-5936
1	General Applied Sciences Lab ATTN: J. Erdos 77 Raynor Ave. Ronkonkama, NY 11779-6649
1	General Electric Company Tactical System Department ATTN: J. Mandzy 100 Plastics Ave. Pittsfield, MA 01201-3698
1	IITRI ATTN: M.J. Klein 10 W. 35th Street Chicago, IL 60616-3799
4	Hercules, Inc. Radford Army Ammunition Plant ATTN: L. Gizzi D.A. Worrell W.J. Worrell C. Chandler Radford, VA 24141-0299

No. of Copies	Organization
2	Hercules, Inc. Allegheny Ballistics Laboratory ATTN: William B. Walkup Thomas F. Farabaugh P.O. Box 210 Rocket Center, WV 26726
1	Hercules, Inc. Aerospace ATTN: R. Cartwright 100 Howard Blvd. Kenville, NJ 07847
1	Hercules, Inc. Hercules Plaza ATTN: B.M. Riggleman Wilmington, DE 19894
1	MBR Research Inc. ATTN: Dr. Moshe Ben-Reuven 601 Ewing St., Suite C-22 Princeton, NJ 08540
1	Olin Corporation Badger Army Ammunition Plant ATTN: F.E. Wolf Baraboo, WI 53913
3	Olin Ordnance ATTN: E.J. Kirschke A.F. Gonzalez D.W. Worthington P.O. Box 222 St. Marks, FL 32355-0222
1	Olin Ordnance ATTN: H.A. McElroy 10101 9th Street, North St. Petersburg, FL 33716
1	Paul Gough Associates, Inc. ATTN: P.S. Gough 1048 South St. Portsmouth, NH 03801-5423
1	Physics International Library ATTN: H. Wayne Wampler P.O. Box 5010 San Leandro, CA 94577-0599

No. of Copies	Organization
2	Princeton Combustion Research Laboratories, Inc. ATTN: N. Mer N.A. Messina Princeton Corporate Plaza 11 Deerpark Dr., Bldg IV, Suite 119 Monmouth Junction, NJ 08852
3	Rockwell International Rocketdyne Division ATTN: BA08, J. Flanagan J. Gray R.B. Edelman 6633 Canoga Avenue Canoga Park, CA 91303-2703
2	Rockwell International Science Center ATTN: Dr. S. Chakravarthy Dr. S. Palaniswamy 1049 Camino Dos Rios P.O. Box 1085 Thousand Oaks, CA 91360
1	Southwest Research Institute ATTN: J.P. Riegel 6220 Culebra Road P.O. Drawer 28510 San Antonio, TX 78228-0510
1	Sverdrup Technology, Inc. ATTN: Dr. John Deur 2001 Aerospace Parkway Brook Park, OH 44142
3	Thiokol Corporation Elkton Division ATTN: R. Willer R. Biddle Tech Library P.O. Box 241 Elkton, MD 21921-0241
1	Veritay Technology, Inc. ATTN: E. Fisher 4845 Millersport Hwy. East Amherst, NY 14501-0305
1	Universal Propulsion Company ATTN: H.J. McSpadden 25401 North Central Ave. Phoenix, AZ 85027-7837

No. of Copies	Organization
1	SRI International Propulsion Sciences Division ATTN: Tech Library 333 Ravenwood Avenue Menlo Park, CA 94025-3493
	Aberdeen Proving Ground
1	Cdr, USACSTA ATTN: STECS-PO/R. Hendricksen

No. of Copies	Organization
1	Ernst-Mach-Institut ATTN: Dr. R. Heiser Haupstrasse 18 Weil am Rheim Germany
1	Defence Research Agency, Military Division ATTN: C. Woodley RARDE Fort Halstead Sevenoaks, Kent, TN14 7BP England
1	School of Mechanical, Materials, and Civil Engineering ATTN: Dr. Bryan Lawton Royal Military College of Science Shrivenham, Swindon, Wiltshire, SN6 8LA England

No. of Copies	Organization
2	Institut Saint Louis ATTN: Dr. Marc Giraud Dr. Gunther Sheets Postfach 1260 7858 Weail am Rhein 1 Germany
1	Explosive Ordnance Division ATTN: A. Wildegger-Gaissmaier Defence Science and Technology Organisation P.O. Box 1750 Salisbury, South Australia 5108
1	Armaments Division ATTN: Dr. J. Lavigne Defence Research Establishment Valcartier 2459, Pie XI Blvd., North P.O. Box 8800 Courcelette, Quebec G0A 1R0 Canada